

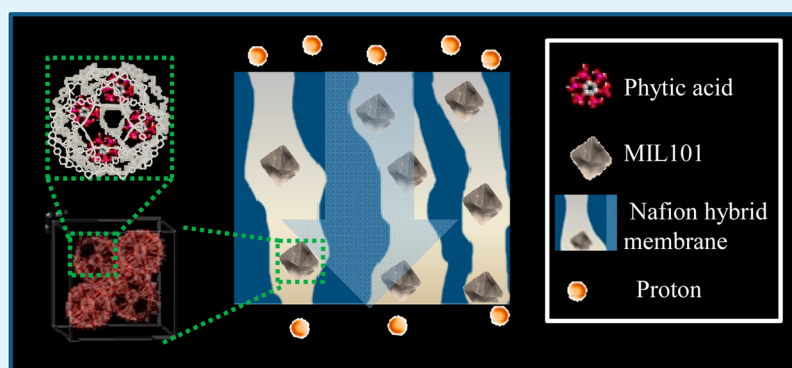
Enhanced Proton Conductivity of Nafion Hybrid Membrane under Different Humidities by Incorporating Metal–Organic Frameworks With High Phytic Acid Loading

Zhen Li,^{†,‡} Guangwei He,^{†,‡} Bei Zhang,^{†,‡} Ying Cao,^{†,‡} Hong Wu,^{†,‡} Zhongyi Jiang,^{*,†,‡} and Zhou Tianian^{†,‡}

[†] Key Laboratory for Green Chemical Technology, Ministry of Education of China, School of Chemical Engineering and Technology, Tianjin University, Tianjin 300072, China

[‡] Collaborative Innovation Center of Chemical Science and Engineering (Tianjin), Tianjin 300072, China

Supporting Information



ABSTRACT: In this study, phytic acid (myo-inositol hexaphosphonic acid) was first immobilized by MIL101 via vacuum-assisted impregnation method. The obtained phytic@MIL101 was then utilized as a novel filler to incorporate into Nafion to fabricate hybrid proton exchange membrane for application in PEMFC under different relative humidities (RHs), especially under low RHs. High loading and uniform dispersion of phytic acid in MIL 101(Cr) were achieved as demonstrated by ICP, FT-IR, XPS, and EDS-mapping. The phytic@MIL101 was dispersed homogeneously in the Nafion matrix when the filler content was less than 12%. Hybrid membranes were evaluated by proton conductivity, mechanical property, thermal stability, and so forth. Remarkably, the Nafion/phytic@MIL hybrid membranes showed high proton conductivity at different RHs, especially under low RHs, which was up to 0.0608 S cm^{-1} and $7.63 \times 10^{-4} \text{ S cm}^{-1}$ at 57.4% RH and 10.5% RH (2.8 and 11.0 times higher than that of pristine membrane), respectively. Moreover, the mechanical property of Nafion/phytic@MIL hybrid membranes was substantially enhanced and the thermal stability of membranes was well preserved.

KEYWORDS: metal–organic framework, MIL101, Nafion, phytic acid, proton exchange membrane, proton conductivity

INTRODUCTION

Proton exchange membrane fuel cell (PEMFC) is one of the most promising energy source for various applications.^{1–3} Current PEMFCs often confront some serious challenges such as catalyst poisoning, low catalyst activity, and complex heat management when operated at low temperature, which could be surmounted by increasing the operating temperature of PEMFCs.^{1,2,4} However, as the heart of PEMFCs, the proton exchange membranes (PEMs) often suffer from sharply declined proton conductivity at elevated temperature because of undesirable dehydration.^{5–7} For instance, Nafion membrane is the most widely used polyelectrolyte membrane and the proton conductivity of Nafion drops off by orders of magnitude with relative humidity (RH) decreasing. Great efforts have been dedicated to developing PEMs with excellent proton conductivity under low RHs, as represented by the following

three approaches. The first approach is the introduction of anhydrous proton-conduction groups into membrane, such as phosphonic acid,^{8,9} imidazole,⁶ and ionic liquids.¹⁰ The second approach is the incorporation of hydrophilic materials to enhance the binding capacity of water of membranes.^{11,12} The third approach is the exploitation of new polyelectrolytes with reduced sensitivity to RH such as block copolymer.^{13,14} The introduction of phosphate groups into membranes combining the first two approaches is deemed quite promising because of the unique superiority of phosphate group such as high charge carrier concentration, high proton conductivity with low dependence on moisture, excellent water retention property,

Received: April 13, 2014

Accepted: June 3, 2014

Published: June 3, 2014

and good thermal stability.^{15,16} Furthermore, phosphate group could act as both proton acceptor and donor by self-dissociation, which is beneficial to forming dynamic hydrogen bond networks and increasing the density of protons at low RHs.¹⁷ Compared with sulfonic acid and imidazole groups, phosphate groups exhibit the highest proton conductivity under low RHs.¹⁸

For stable and long-term utilization of phosphate groups, phosphate group donating molecules should be in immobilized form rather than in free form, which required to find a suitable match between supporter and phosphate group donating molecules (guest molecules). The immobilization of guest molecules on supporters has been widely explored in many fields like enzyme catalysis,¹⁹ heterogeneous catalysis.^{20,21} Some principles could be summarized for choosing ideal supporters and guest molecules: (1) large amount of active sites in guest molecules and high load capacity of supporters; (2) good chemical stability, thermal stability for guest molecules, and high mechanical stability for supporters as well; (3) modest interaction between guest molecules and supporters; (4) easy availability of active sites of guest molecules within the supporters. Based on above principles, phytic acid (myo-inositol hexakisphosphate, Figure 1) and MIL101 (Figure 2)

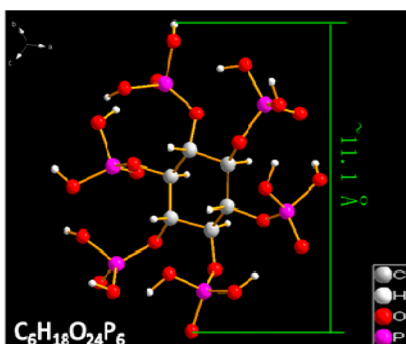


Figure 1. Molecule structure of phytic acid.

were employed as guest molecules (phosphate group donation molecule) and supporter in this study, respectively. Phytic acid is obtained from plants with unique properties such as the highest phosphate groups content (except phosphoric acid), excellent iron-chelating ability, good chemical, and thermal stabilities.^{22–24} The molecular diameter of phytic acid is ~ 1.1 nm, which is similar to the window diameter of cavities in MIL101, indicating that phytic acid could be confined by those cavities effectively. Meanwhile, there are abundant coordinatively unsaturated metal sites (CUS) in MIL101, which could be chelated by phytic acid, resulting in moderate interaction between phytic acid and MIL101.^{25,26} It can be expected that phytic acid could be immobilized in MIL101 with a low leakage ratio. As a kind of porous coordination polymer, MIL101 possesses open-framework structure, which ensures the availability of active sites in phytic acid for rapid proton transfer. In addition, MIL101 is endowed with potential of high load capacity for phytic acid because of its unique characters like gigantic pore volume of $1.5\text{--}1.9\text{ cm}^3\text{ g}^{-1}$, huge Langmuir surface area of $\sim 5900 \pm 300\text{ m}^2\text{ g}^{-1}$ and good stability.²⁷

Herein, we impregnated phytic acid into MIL101 by vacuum-assisted method (VAM) and the corresponding Nafion/MIL101 hybrid membranes were prepared using phytic@MIL101 as the novel filler. Phytic acid was dispersed homogeneously in MIL101 and the loading content of phytic acid in MIL101 was up to about 12 wt %. The Nafion/MIL101 hybrid membranes showed good proton conductivity at different RHs, especially under low RHs, which was 1100% higher than that of pristine membrane at 10.5% RH.

■ MATERIALS AND METHODS

Synthesis, Purification of MIL101, and Impregnation of Phytic Acid into MIL101. MIL101(Cr) was synthesized and purified as described in previous study.^{27,28} MIL101 was synthesized by hydrothermal method. When the reaction finished, solid was separated, which was a mixture of MIL101, crystalline terephthalic acid, and few chromic nitrate. DMF was employed to dissolve the residual crystalline terephthalic acid and chromic nitrate at room temperature and MIL101 was left, which was named as raw-MIL101. Raw-MIL101 was treated by DMF for 12 h 3 times under reflux to

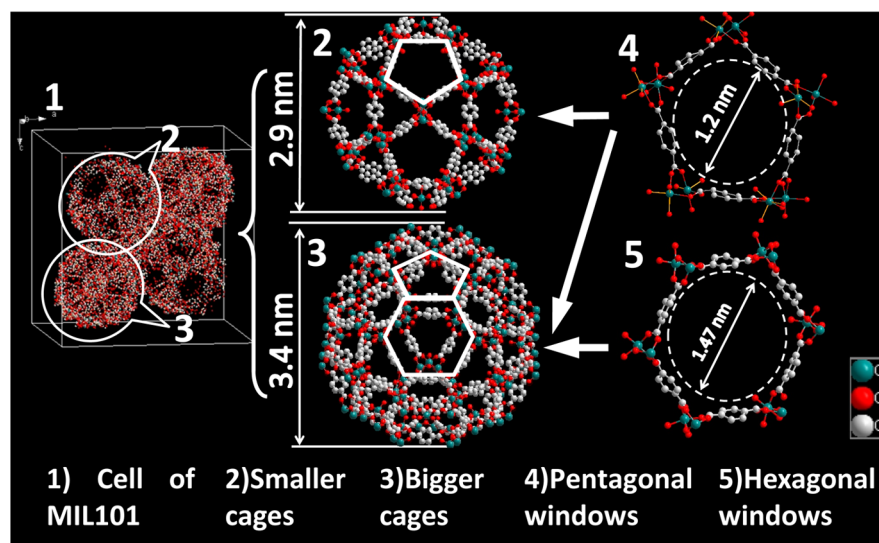


Figure 2. Structure of MIL101: MIL101 is constructed by two types of rigid quasi-spherical cavities with diameter of 2.9 nm for small and 3.4 nm for big. The small cavities are only constructed by 1.2 nm pentagonal windows, and the big cavities own are constructed both the same pentagonal windows and 1.5 nm hexagonal windows.²⁷

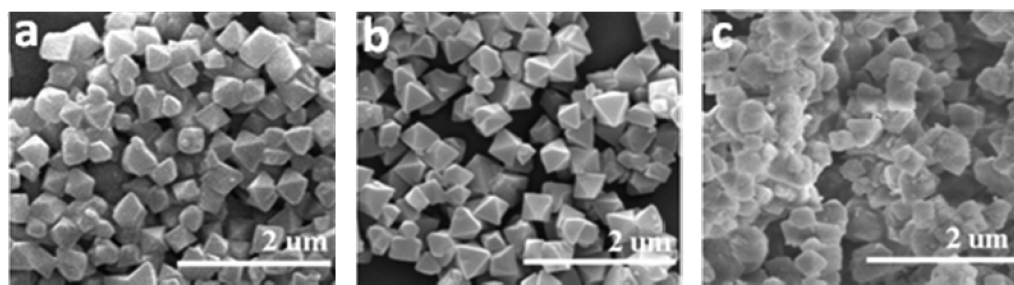


Figure 3. FESEM images of raw-MIL101 (a), pure-MIL101 (b), and phytic@MIL101 (c).

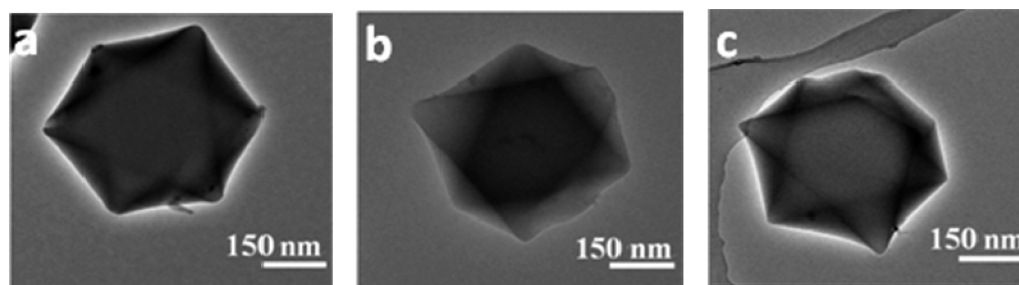


Figure 4. FETEM images of raw-MIL101 (a), pure-MIL101 (b), and phytic@MIL101 (c).

remove terephthalic acid in their pores, and treated by 1 M ammonium fluoride for 12 h 3 times under reflux. For reducing the difficulty of vacuum-pumping in next step, the raw-MIL101 was then treated by EtOH and dichloromethane for 12 h under reflux to replace the high boiling point solvents by low one. The product was named as pure-MIL101.

Phytic acid was impregnated into MIL101 via VAM by the following steps.⁴ First, pure-MIL101 was treated in a Schlenk tube under vacuum at 120 °C for 12 h to remove the trace of residual dichloromethane and trapped air in pores. Second, the Schlenk tube was cooled to 80 °C. Water (20 mL) and phytic acid aqueous solution (20 mL) were added into the Schlenk tube under vacuum. Third, vacuum was removed and the mixture was stirred for 24 h. Phytic acid could be pressed into the cavities of MIL101 by the pressure difference between the cavities and atmosphere. Fourthly, the treated pure-MIL101 was centrifuged from the mixture, washed by water until the pH of supernatant liquid was neutral, and dried at 45 °C under vacuum until constant weight. Finally, a celadon powder could be obtained, which was designed as phytic@MIL101.

Preparation of Membranes. The membranes were prepared by solution-casting method. The received Nafion solution was evaporated at 60 °C under vacuum for 24 h to obtain dry Nafion resin. The obtained Nafion resin (0.2 g) was redissolved in DMAc (4 mL) and a desired amount of phytic@MIL101 or pure-MIL101 was dispersed into the solution homogeneously. The mixture was cast onto a glass plate, kept at 80 °C for 12 h, and then kept at 120 °C for another 4 h. Through immersing the glass plate in water, the membranes were peeled off.

Recasting Nafion membrane must be activated before used. All membranes were soaked in aqueous oxyful (3 wt %), rinsed in water, and soaked in sulfuric acid (aqueous solution, 1 mol L⁻¹), successively, and each aforementioned operation was carried out at 80 °C for 1 h. Subsequently, the membranes were washed by water until the pH was neutral. The hybrid membranes were named after Nafion/phytic@MIL-X or Nafion/pure-MIL-X, where phytic@MIL or pure-MIL referred to the filler in hybrid membranes, respectively, and X referred to the weight percentage of phytic@MIL101 or pure-MIL101 relative to Nafion. Nafion pristine membrane was prepared and activated by the same procedures for comparison purpose and named after pristine Nafion membrane.

Leakage Ratio of Phytic Acid in Dynamic Condition. The leakage ratio of phytic acid was tested in periodic-replacement water at

80 °C. Phytic@MIL101 (0.05 g) was immersed in 10 mL deionized water at 80 °C for 4.5 days, and then phytic@MIL101 was centrifuged from supernatant liquid. The obtained phytic@MIL101 was immersed in 10 mL fresh deionized water at 80 °C for another 4.5 days and the supernatant liquid was tested by ICP to detect the content of phosphorus element. The aforementioned procedures were in loop execution. The leakage ratio of phytic acid was calculated by the following equations (eqs 1 and 2).

$$m_n = V \frac{\omega_n M_{\text{phy}}}{6M_p} \quad (1)$$

$$L_n = \frac{(\sum_{j=1}^n m_j)}{0.05\omega_p} \quad (2)$$

where ω_n (wt %, g mL⁻¹) is the content of phosphorus element of supernatant liquid separated after the n th circle, V is the volume of water (10 mL), M_{phy} (g mol⁻¹), and M_p (g mol⁻¹) are relative molecular mass of phytic acid and relative atomic mass of phosphorus, respectively, m_n (g) is the leakage of phytic acid in the n th circle, Σ is a summation notation and is employed to calculate the total leakage of phytic acid after the n th circle, ω_p (wt %, g g⁻¹) is the phytic acid content of phytic@MIL101 determined by ICP as described in section characterizations of MIL101, L_n (%) is leakage ratio of phytic acid after the n th circle.

Proton Conductivity of Membranes. To explore the potential application of membranes for PEMFCs at low RHs, proton conductivity of membranes (σ , S cm⁻¹) at different temperatures and different RHs were investigated using AC impedance spectroscopy.

Proton conductivity at different temperatures was obtained by the same way as reported in our previous study.²⁹

Proton conductivity at different RHs was obtained in the same method except the test condition was controlled at 80 °C and a series of RHs. A two point platinum probe cell was placed in a stainless steel container (cubage = 1.5 L) at 80 °C. Humidity was controlled by the following saturated salt solution in a chamber placed in the stainless steel container: LiCl (RH = 10.5%), KAc (RH = 15.1%), MgCl₂ (RH = 26.1%), K₂CO₃ (RH = 41.1%), and NaNO₂ (RH = 57.4%). Each sample was equilibrated in controlled environment for at least 6 h until the impedance of sample was constant. The proton conductivity was obtained by the same way as that at 100% RH.

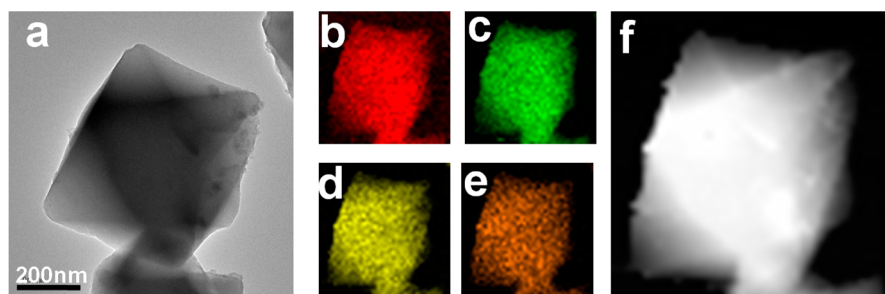


Figure 5. Elemental distribution of phytic@MIL101 probed by EDS-mapping: (a) FETEM image of phytic acid; (b) distribution of carbon; (c) distribution of chromium; (d) distribution of oxygen; (e) distribution of phosphorus; (f) STEM image display HAADF detector.

RESULTS AND DISCUSSION

Characterization of MIL101. Morphology of MIL101 was observed by FESEM and FETEM, and the results are shown in Figures 3 and 4, respectively. Approximate octahedral crystals with a uniform size of about 450 nm could be observed. By comparing Figure 2, it could be concluded that the morphology of octahedral crystals was not altered by the purification process and degasification process, but it was altered by the impregnation of phytic acid. FETEM images revealed the morphology of MIL101. The octahedral shape of MIL101 was not changed after purification process, but horns of MIL101 were slightly damaged by impregnation of phytic acid afterward.

XRD was employed to determine the crystal structures of raw-MIL101, pure-MIL101, and phytic@MIL101. XRD patterns of MIL101 are shown in Figure 5 together with the simulated XRD pattern of MIL101, which were simulated from the.cif file supplied by Cambridge crystallographic data center (CCDC). The comparison between patterns in Figure 5 revealed that a pure phase MIL101 was synthesized successfully and the crystal structure of MIL101 was unaffected after purification, degasification, and impregnation processes.

The successful impregnation of phytic acid was confirmed by EDX, XPS, and FT-IR. The EDX result verified the presence of a considerable amount of phosphorus element (P). The spectra of FT-IR demonstrated the presence of phytic acid. The peaks at 1142 and 1058 cm^{-1} could be corresponded to the stretching vibrations of —P=O and phosphate ester group (P—O—C), respectively.¹⁵ New peaks appearing at 611 cm^{-1} reveal the existence of chelation between phytic acid and CUSs.³⁰ The peak at 1690 cm^{-1} could be relevant to the flexural vibration of bonded water (H—O—H),³⁰ indicating that water molecules were bound by phytic acid. XPS was performed to determine P content in surface layer of MIL101 and the oxidation state of P. The peak of binding energy at around 131.5 eV indicated the pentavalent-oxidation state of P and the presence of P—O bond. The content of P element in surface-layer of MIL101 (4–10 nm depth) could be calculated by the peak area ratio, which was 3.61 wt %. The content of P element in entire MIL101 was measured by ICP and the results was 3.69 wt %, indicating 11.54 wt % of phosphate groups was immobilized in MIL101. The spectra corresponding to these configurations can be found in the Supporting Information.

The distribution of phytic acid in MIL101 was observed by the result of EDS-mapping and inferred by the comparison between the result of ICP and XPS. The result of EDS-mapping in Figure 5 revealed the distribution of P in phytic@MIL101, with the distribution of carbon (C), chromium (Cr), and oxygen (O) as comparison. It could be clearly observed that P was of uniform distribution, which was further confirmed by the

similar P content in the entire MIL101 (3.69 wt %, detected by ICP) and in the surface layer of MIL101 (3.61 wt %, detected by XPS).

Leakage Ratio of Phytic Acid from phytic@MIL101.

The leakage ratio of phytic acid was calculated to evaluate phytic acid retention property of phytic@MIL101 in water at 80 °C, as shown in Figure 6. The leakage ratio of phytic acid

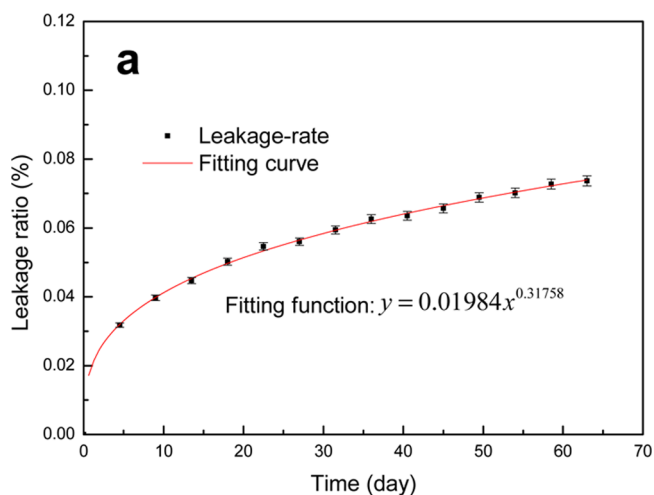


Figure 6. Leakage ratio curve of phytic acid.

increased over time while the leakage rate of phytic acid decreased. The functional relationship between leakage ratio and time fitted a power function with a formula of $y = 0.01984x^{0.31758}$, where y was the leakage ratio and x was time. The fitting curve showed a high coefficient of determination of 0.99751, indicating that the fitting was reasonable. It could be deduced from the leakage ratio formula that the leakage ratio was 12.920%, 26.844%, and 30.534% after 1, 10, and 15 years, respectively. In comparison, H_3PO_4 @MIL101 was prepared in previous literature and about 95% of acid leaked out after 20 min.³¹ The low leakage ratio can be attributed to two factors. (i) The similar diameter between phytic acid and the windows in MIL101. (ii) Chelation between phytic acid and CUSs. As to low RHs, the leakage ratio was significantly lower than that in water under identical temperature. Hence, phytic@MIL101 is suitable for the application in PEMFC (whose service life span is about 10 years).

Thermal Stability of MIL101 and Membranes. TGA of MIL101 was performed to investigate their thermal stability, as shown in Figure 7. The decomposition process of pure-MIL101 could be divided into three sections. The trace of weight loss between 50 and 150 °C was caused by the bound water and

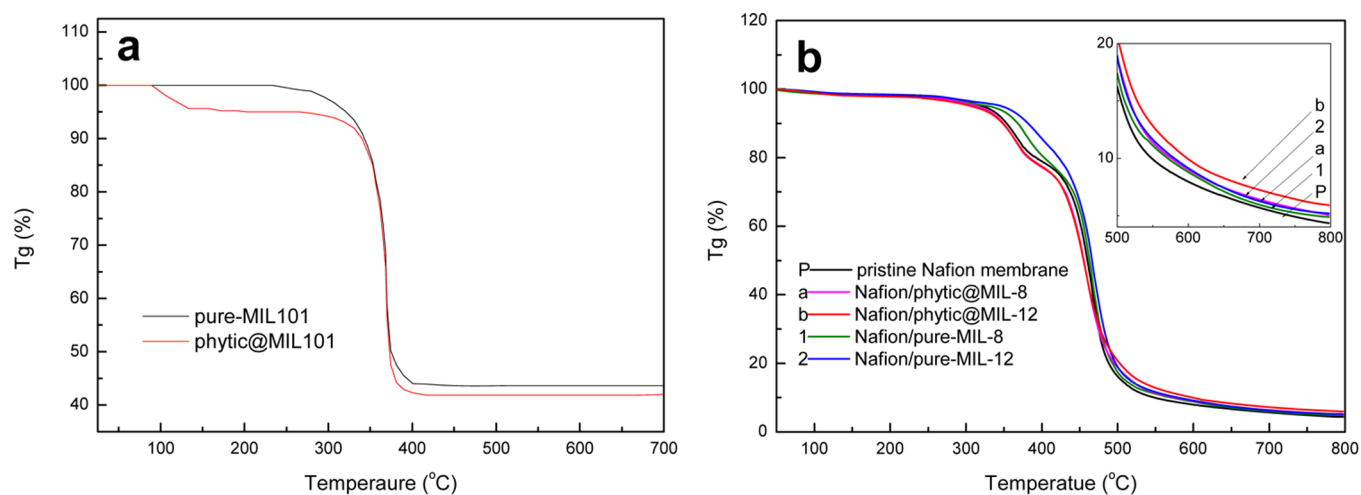


Figure 7. Thermal stability analysis of MIL101 and membranes: (a) the TGA curve of raw-MIL101 and phytic@MIL101; (b) the TGA curve of membranes.

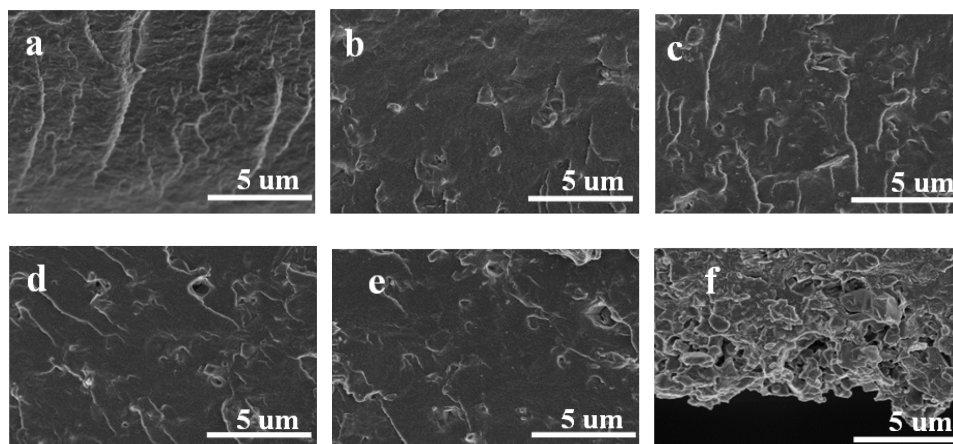


Figure 8. FESEM images of the cross-section of membranes: (a) pristine Nafion membrane; (b) Nafion/pure-MIL-8; (c) Nafion/pure-MIL-12; (d) Nafion/phytic@MIL-8; (e) Nafion/phytic@MIL-12; (f) Nafion/phytic@MIL-16.

residual solvent like free-water and DMF. The weight was constant at the temperature range of 150 to 300 °C because the water and residual solvent exhausted. The pure-MIL101 remained stable until 300 °C, and then the weight decreased sharply from 300 to 500 °C, which was due to the decomposition of skeleton of MIL101.²⁷ Because of the nonvolatility of CrO_x , the weight remained nearly constant in last section above 550 °C. Phytic@MIL101 displayed a similar decomposition process as pure-MIL101 except for the following details. The weight loss of about 4.4% was more obvious than that of pure-MIL101 at the temperature range from 100 to 150 °C. Considering the boiling point of phosphoric acid and inositol (which were products of the decomposition of phytic acid) was 158 °C (decomposition) and 225–227 °C, the weight loss was not ascribed to the decomposition or volatilization of phytic acid but ascribed to the loss of bound water. The existence of large amount of bound water in phytic@MIL101 benefited from the extensive hydrogen bonding of phytic acid with water. The large amount of bound water also implied good proton conductivity of phytic@MIL101 under low RHs. No another obvious weight loss was found below 250 °C, indicating that the phytic acid could not decomposed below 250 °C in MIL101. The total weight loss of phytic@MIL101 was 2.8% higher than that of

pure-MIL101, which was caused by the volatilization of bound water. Thus, phytic@MIL101 cannot be decomposed below 300 °C, indicating that phytic@MIL101 was stable enough to bear the application conditions of PEMFCs.

TGA of membranes was carried out to investigate the influence of incorporation of MIL101 on the thermal stability of membranes. It could be concluded that the thermal decomposition process of membranes was scarcely affected by the incorporation of MIL101, indicating that the thermal stability of membranes was maintained. The total weight loss decreased with the increasing content of MIL101, and the weight loss of hybrid membranes was slower than that of pristine membrane, which was caused by that CrO_x was nonvolatile, and it could act as a barrier retarding the escape of other volatile substances.^{32,33}

Characterization of Membranes. The morphology of membranes (Figure 8) was observed by probing cross sections of membranes using FESEM. The membranes were dense without obvious defect. Because the Nafion polymer chains were very flexible, the MIL101 was wrapped tightly by the chains of Nafion, resulting in good compatibility between MIL101 and Nafion matrix. Both pure-MIL101 and phytic@MIL101 were uniformly dispersed in hybrid membranes at the

filler contents below 12 wt %. However, serious agglomeration occurred at the filler content of 16 wt %.

FR-IR of membranes was carried out to determine the interactions between Nafion matrix and phytic@MIL (Figure 9). Peaks at 1628 and 3559 cm^{-1} (related to the S–O–H

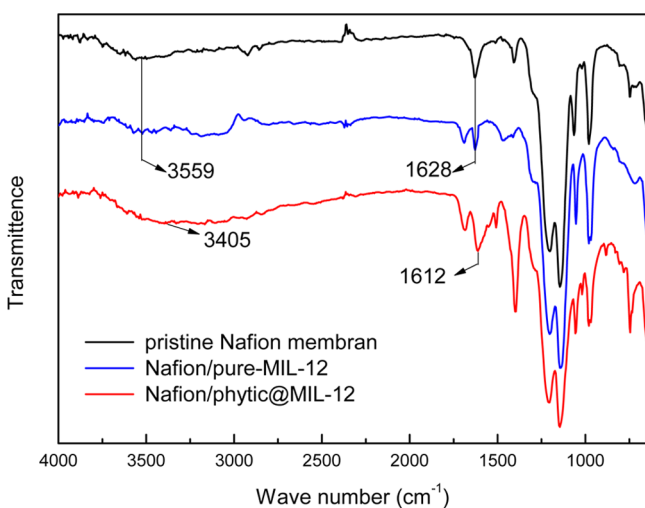


Figure 9. FT-IR spectrum of membranes.

groups in Nafion) were shifted to low wavenumber (1612 and 3478 cm^{-1} , respectively), indicating that hydrogen bonding was formed between sulfuric group and phytic acid after the incorporation of phytic@MIL.

Water Uptake and Area Swelling of Membranes.

Figure 10 displayed that pristine Nafion membrane showed a high area swelling from 25.68% to 59.62% with the increased temperature from 20 to 80 °C. The incorporation of either phytic@MIL101 or pure-MIL101 restrained the area swelling of membranes effectively. For instance, the highest decrement ratios of area swelling reached 61.76% and 68.26% after the incorporation of phytic@MIL101 and pure-MIL101 at 20 °C, respectively. The variation tendency of water uptake was in accordance with that of area swelling. Apparent activation energies of area swelling and water uptake (E_a and E_{a_u}) were derived from their Arrhenius plots, as shown in Table 1. Both

E_a and E_{a_u} of hybrid membranes were higher than those of pristine Nafion membrane. It was attributed to the fact that the framework of MIL101 is rigid, which could not swell in water.^{34,35} In addition, MIL101 constrained the swelling of polymer matrix via constraining motions of polymer chains, as confirmed by the result of DSC. Similarly, it was difficult for MIL101 to absorb as much water as polymers by swelling.³⁵ As a result, all hybrid membranes showed higher resistance to area swelling and water uptake than pristine Nafion membrane. As the filler content increasing, more rigid MIL101 was introduced into membranes, hybrid membranes exhibited increased E_a and E_{a_u} as well as further decreased area swelling and water uptake. Compared with Nafion/pure-MIL hybrid membranes, Nafion/phytic@MIL hybrid membranes showed lower E_a and E_{a_u} . This was caused by that the hydrogen bonding could form between phytic acid and other hydroxy compounds, which was not only from the sulfuric acid groups in Nafion but also from water molecules.

Activation Energy of Proton Conductivity of Membranes. Proton conductivity is a key parameter for a PEM determining fuel cell performance. Proton conductivity at different temperatures was measured to evaluate the influence of incorporated MIL101 on activation energy of proton conductivity, as illustrated in Figure 11. It could be concluded that there was positive correlation between proton conductivity and temperature, indicating that proton conduction was a thermally activated process. All the hybrid membranes showed higher proton conductivity compared with pristine Nafion membrane. Nafion/Phytic@MIL-12 possessed the highest proton conductivity, which was about 45% higher than pristine Nafion membrane in whole temperature range. Activation energy of pristine Nafion membrane was 16.96 kJ mol^{-1} . The incorporation of MIL101 decreased the activation energy of hybrid membranes, which was decreased to about 15 kJ mol^{-1} for Nafion/phytic@MIL hybrid membranes and 16 kJ mol^{-1} for Nafion/pure-MIL hybrid membranes, suggesting the resistance of proton transfer was decreased by incorporating MIL101. The reduced activation energy can be interpreted as follows.

MIL101 was a kind of Lewis acid due to the abundant CUSs.²⁶ Large number of hydroxyl groups and H^+ can be

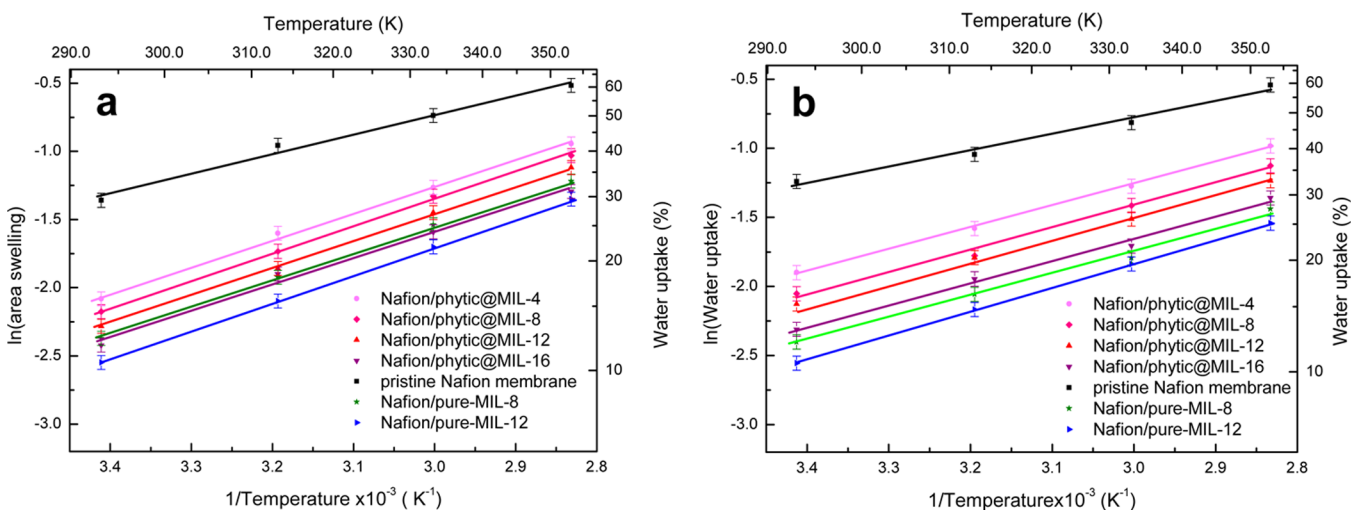


Figure 10. Arrhenius plot of area swelling (a) and water uptake (b) of membranes.

Table 1. Apparent Activation Energy of Area Swelling and Water Uptake of Membranes

activation energy (kJ mol ⁻¹)	pristine	Nafion/phytic@MIL-X				Nafion/pure-MIL-X	
		X = 4	X = 8	X = 12	X = 16	X = 8	X = 12
E_{a_s}	11.88 ± 0.30	16.15 ± 0.40	16.55 ± 0.41	16.81 ± 0.42	15.95 ± 0.39	16.94 ± 0.42	17.45 ± 0.44
E_{a_w}	9.94 ± 0.25	13.12 ± 0.33	13.48 ± 0.34	13.87 ± 0.35	12.49 ± 0.31	13.91 ± 0.35	14.51 ± 0.36

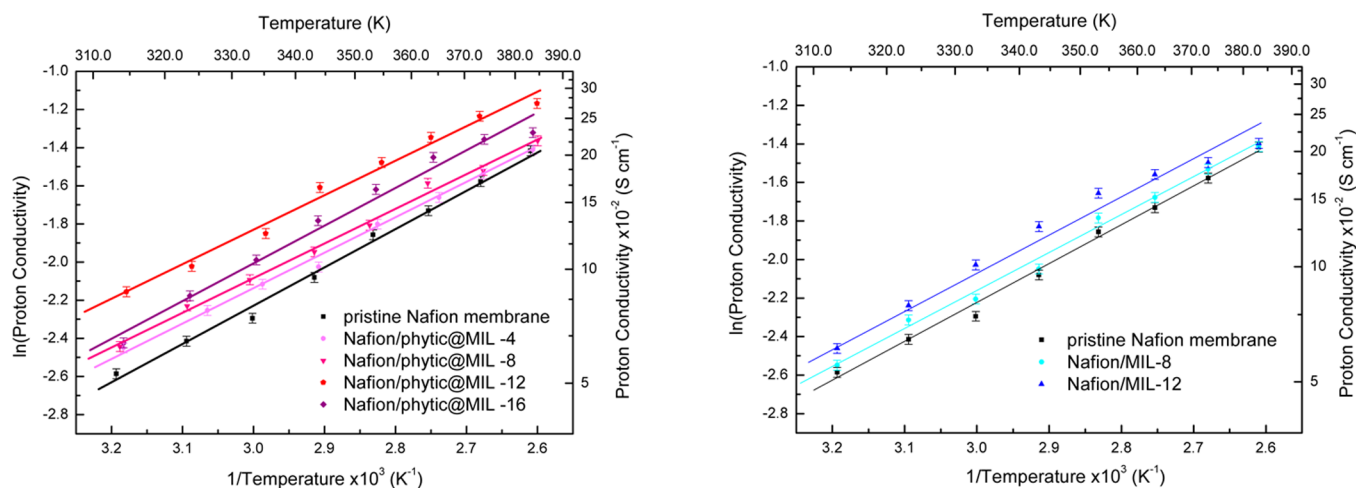


Figure 11. Arrhenius plot of proton conductivity membranes.

Table 2. Apparent Activation Energy of Proton Conductivity of Membranes

activation energy (kJ mol ⁻¹)	pristine	Nafion/phytic@MIL-X				Nafion/pure-MIL-X	
		X = 4	X = 8	X = 12	X = 16	X = 8	X = 12
E_a	16.96 ± 0.42	15.15 ± 0.38	15.08 ± 0.37	15.14 ± 0.38	16.39 ± 0.41	16.29 ± 0.40	15.81 ± 0.39

created by hydrolyzing the CUSs, which were capable of increasing membrane acidity and facilitating the construction of dynamic hydrogen bonding networks for proton transfer in pores of MIL101, leading to decreased activation energy.^{36–38}

As to phytic@MIL101, the acidity of phosphate groups is stronger than CUSs, and the acidity of Nafion/phytic@MIL hybrid membrane can be further enhanced for facile proton transport. In addition, since the high hydrogen bonding energy of phosphate groups, phytic acid possessing high density of phosphate groups could exhibit strong interaction with water molecules and sulfuric acid, which helped to construct dynamic hydrogen-bonded networks to facilitate the proton conductivity by Grotthuss mechanism.^{22,24} Thus, the incorporation of phytic@MIL101 showed lower activation energy and exhibited higher proton conductivity than both pristine Nafion membrane and Nafion/pure-MIL hybrid membranes.

Proton Conductivity of Membranes in Different RHs.

The proton conductivity dependence on RH of all the membranes was illustrated in Figure 12. Pristine Nafion membrane displayed the highest sensitivity to the RH, and the proton conductivity declined from 0.156 S cm⁻¹ at 100% RH to 6.36 × 10⁻⁵ S cm⁻¹ at 10.5% RH. The proton conductivity of hybrid membranes was enhanced by incorporating phytic@MIL101 and the enhancement increased along with decreased RH. Nafion/phytic@MIL-12 exhibited the best proton conductivity of 0.228 S cm⁻¹ at 100% RH, 0.0608 S cm⁻¹ at 57.4% RH and 7.63 × 10⁻⁴ S cm⁻¹ at 10.5% RH, which was 0.46, 2.8, and 11.0 times higher than that of pristine membrane, respectively. On the contrary, the incorporation of pure-MIL101 decreased the proton conductivity of hybrid

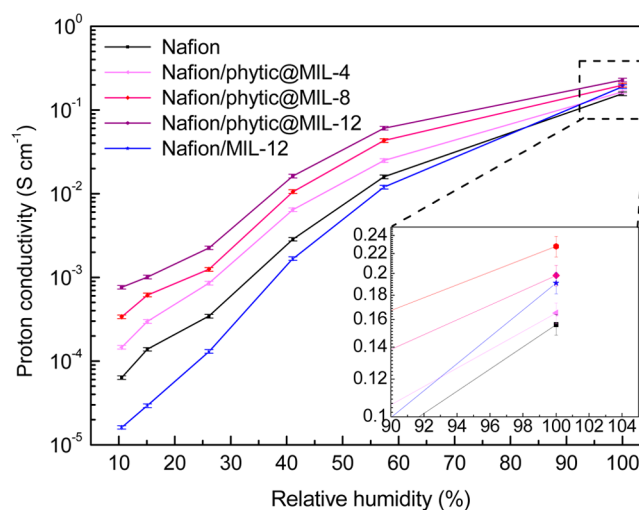


Figure 12. Proton conductivity of membranes under different RHs at 80 °C.

membrane under reduced RH. As discussed in the section activation energy of proton conductivity of membranes, the proton conductivity of Nafion/pure-MIL hybrid membranes showed higher proton conductivity than pristine Nafion membrane at 100% RH, which was due to the construction of dynamic hydrogen bonding networks in pure-MIL101 afforded by hydrolyzing the CUSs. As the RH decreased, it is difficult for the CUSs to be fully hydrolyzed, resulting in weakened proton conduction capacity of pure-MIL101. The remarkable enhancement of proton conductivity by the

incorporation of phytic@MIL-X can be interpreted as follows: (i) numerous phosphate groups were immobilized in the regular frameworks of MIL101, rendering continuous channels for facile proton transport; (ii) phosphate group possesses a less proton-conduction dependence on water, and exhibit the best proton conductivity under low RHs in comparison with sulfuric acid and imidazole groups;^{16,18} (iii) as to phosphate proton conductor, high mobility of phosphate groups is essential to unleashing their proton conduction potential;⁸ in phytic@MIL101, phytic acid was immobilized not by covalent bonds but by coordinated bonds and cage effect, which has relatively high mobility to maintain its excellent proton conductivity; (iv) one phytic acid molecule has six phosphate groups. Such a molecule structure with high concentration of phosphate groups may render proton transport rapid.

CONCLUSIONS

In this study, we immobilized phytic acid in MIL101 in order to gain a stable and long-term utilization of phosphate groups. Due to the similar diameter between phytic acid and the windows in MIL101 as well as the chelation between phytic acid and CUSs, the phytic@MIL101 exhibited an low phytic acid leakage ratio. Using phytic@MIL101 as the novel filler, Nafion/phytic@MIL hybrid membranes were prepared which displayed excellent proton conductivity under different RHs, especially under low RHs. For instance, the proton conductivity was up to 0.0608 S cm^{-1} and $7.63 \times 10^{-4} \text{ S cm}^{-1}$ at 57.4% RH and 10.5% RH (2.8 and 11.0 times higher than that of pristine membrane), respectively. This remarkable enhancement in proton conductivity was mainly ascribed to the unique properties of phytic acid and the good match between phytic acid and MIL101: (i) with the regular frameworks of MIL101, continuous channels could be formed by the immobilized phosphate groups for facile proton transport; (ii) with a less proton-conduction dependence on water, phosphate groups exhibited the high proton conductivity under low RHs; (iii) high mobility of phosphate groups in the cavities of MIL101 ensured rapid proton conduction potential; (iv) high concentration of phosphate groups of phytic acid rendered massive proton transport. Moreover, mechanical and swelling-resistance properties of the hybrid membrane were improved. The developed hybrid membrane showed great potential for application in PEMFC.

ASSOCIATED CONTENT

Supporting Information

More experimental details and additional experimental data including spectrum of EDX, FT-IR, XPS; the BET results of MIL101; DSC measurement of membranes; and mechanical property of membranes. This material is available free of charge via the Internet at <http://pubs.acs.org>.

AUTHOR INFORMATION

Corresponding Author

*Fax: +86 22 2350 0086. Tel: +86 22 2350 0086. E-mail: zhyjiang@tju.edu.cn.

Author Contributions

The manuscript was written through contributions of all authors. All authors have given approval to the final version of the manuscript.

Notes

The authors declare no competing financial interest.

ACKNOWLEDGMENTS

We gratefully acknowledge financial support from National Science Fund for Distinguished Young Scholars (21125627), the National High Technology Research and Development Program of China (2012AA03A611), and the Program of Introducing Talents of Discipline to Universities (No. B06006).

REFERENCES

- (1) Lee, H. J.; Kim, J. H.; Won, J. H.; Lim, J. M.; Hong, Y. T.; Lee, S. Y. Highly Flexible, Proton-Conductive Silicate Glass Electrolytes for Medium-Temperature/Low-Humidity Proton Exchange Membrane Fuel Cells. *ACS Appl. Mater. Interfaces* **2013**, *5*, 5034–5043.
- (2) Lu, F.; Gao, X.; Yan, X.; Gao, H.; Shi, L.; Jia, H.; Zheng, L. Preparation and Characterization of Nonaqueous Proton-Conducting Membranes with Protic Ionic Liquids. *ACS Appl. Mater. Interfaces* **2013**, *5*, 7626–7632.
- (3) Hickner, M. A.; Ghassemi, H.; Kim, Y. S.; Einsla, B. R.; Mcgrath, J. E. Alternative Polymer Systems for Proton Exchange Membranes (PEMs). *Chem. Rev.* **2004**, *104*, 4587–4611.
- (4) Lu, S.; Wang, D.; Jiang, S. P.; Xiang, Y.; Lu, J.; Zeng, J. HPW/MCM-41 Phosphotungstic Acid/Mesoporous Silica Composites as Novel Proton-Exchange Membranes for Elevated-Temperature Fuel Cells. *Adv. Mater.* **2010**, *22*, 971–976.
- (5) Wang, J.; Yue, X.; Zhang, Z.; Yang, Z.; Li, Y.; Zhang, H.; Yang, X.; Wu, H.; Jiang, Z. Enhancement of Proton Conduction at Low Humidity by Incorporating Imidazole Microcapsules into Polymer Electrolyte Membranes. *Adv. Funct. Mater.* **2012**, *22*, 4539–4546.
- (6) Park, C. H.; Lee, C. H.; Guiver, M. D.; Lee, Y. M. Sulfonated Hydrocarbon Membranes for Medium-Temperature and Low-Humidity Proton Exchange Membrane Fuel Cells (PEMFCs). *Prog. Polym. Sci.* **2011**, *36*, 1443–1498.
- (7) Zhang, H.; Shen, P. K. Recent Development of Polymer Electrolyte Membranes for Fuel Cells. *Chem. Rev.* **2012**, *112*, 2780–2832.
- (8) Lee, S.-I.; Yoon, K.-H.; Song, M.; Peng, H.; Page, K. A.; Soles, C. L.; Yoon, D. Y. Structure and Properties of Polymer Electrolyte Membranes Containing Phosphonic Acids for Anhydrous Fuel Cells. *Chem. Mater.* **2012**, *24*, 115–122.
- (9) Umeyama, D.; Horike, S.; Inukai, M.; Itakura, T.; Kitagawa, S. Inherent Proton Conduction in A 2D Coordination Framework. *J. Am. Chem. Soc.* **2012**, *134*, 12780–12785.
- (10) Subianto, S.; Mistry, M. K.; Choudhury, N. R.; Dutta, N. K.; Knott, R. Composite Polymer Electrolyte Containing Ionic Liquid and Functionalized Polyhedral Oligomeric Silsesquioxanes for Anhydrous PEM Applications. *ACS Appl. Mater. Interfaces* **2009**, *1*, 1173–1182.
- (11) He, G. W.; Li, Z. Y.; Li, Y. F.; Li, Z.; Wu, H.; Yang, X. L.; Jiang, Z. Y. Zwitterionic Microcapsules as Water Reservoirs and Proton Carriers Within Nafion Membrane to Confer High Proton Conductivity under Low Humidity. *ACS Appl. Mater. Interfaces* **2014**, DOI: 10.1021/Am500626f.
- (12) Wang, J.; Zhang, H.; Yang, X.; Lv, W.; Jiang, Z.; Qiao, S. Z. Enhanced Water Retention by Using Polymeric Microcapsules To Confer High Proton Conductivity On Membranes at Low Humidity. *Adv. Funct. Mater.* **2011**, *21*, 971–978.
- (13) Higashihara, T.; Matsumoto, K.; Ueda, M. Sulfonated Aromatic Hydrocarbon Polymers as Proton Exchange Membranes for Fuel Cells. *Polymer* **2009**, *50*, 5341–5357.
- (14) Matsumoto, K.; Higashihara, T.; Ueda, M. Star-Shaped Sulfonated Block Copoly(Ether Ketone)s as Proton Exchange Membranes. *Macromolecules* **2008**, *41*, 7560–7565.
- (15) He, G.; Nie, L.; Han, X.; Dong, H.; Li, Y.; Wu, H.; He, X.; Hu, J.; Jiang, Z. Constructing Facile Proton-Conduction Pathway Within Sulfonated Poly(Ether Ether Ketone) Membrane by Incorporating Poly(Phosphonic Acid)/Silica Nanotubes. *J. Power Sources* **2014**, *259*, 203–212.
- (16) Schuster, M.; Rager, T.; Noda, A.; Kreuer, K. D.; Maier, J. About the Choice of the Protogenic Group in PEM Separator Materials for Intermediate Temperature, Low Humidity Operation: A Critical

Comparison of Sulfonic Acid, Phosphonic Acid, and Imidazole Functionalized Model Compounds. *Fuel Cells* **2005**, *5*, 355–365.

(17) Vilčiauskas, L.; Tuckerman, M. E.; Bester, G.; Paddison, S. J.; Kreuer, K.-D. The Mechanism of Proton Conduction in Phosphoric Acid. *Nat. Chem.* **2012**, *4*, 461–466.

(18) Paddison, S. T.; Kreuer, K. D.; Maier, J. About the Choice of the Protogenic Group in Polymer Electrolyte Membranes: Ab initio Modelling of Sulfonic Acid, Phosphonic Acid, and Imidazole Functionalized Alkanes. *Phys. Chem. Chem. Phys.* **2006**, *8*, 4530–4542.

(19) Magner, E. Immobilisation of Enzymes on Mesoporous Silicate Materials. *Chem. Soc. Rev.* **2013**, *42*, 6213–6222.

(20) Mcmorn, P.; Hutchings, G. J. Heterogeneous Enantioselective Catalysts: Strategies for the Immobilization of Homogeneous Catalysts. *Chem. Soc. Rev.* **2004**, *33*, 108–122.

(21) Thomas, J. M.; Raja, R. Exploiting Nanospace for Asymmetric Catalysis: Confinement of Immobilized, Single-Site Chiral Catalysts Enhances Enantioselectivity. *Acc. Chem. Res.* **2008**, *41*, 708–720.

(22) Mistry, M. K.; Choudhury, N. R.; Dutta, N. K.; Knott, R.; Shi, Z.; Holdcroft, S. Novel Organic–Inorganic Hybrids with Increased Water Retention for Elevated Temperature Proton Exchange Membrane Application. *Chem. Mater.* **2008**, *20*, 6857–6870.

(23) Su, J.; Wu, X.-L.; Yang, C.-P.; Lee, J.-S.; Kim, J.; Guo, Y.-G. Self-Assembled LiFePO_4/C Nano/Microspheres by Using Phytic Acid as Phosphorus Source. *J. Phys. Chem. C* **2012**, *116*, 5019–5024.

(24) Crea, F.; De Stefano, C.; Milea, D.; Sammartano, S. Formation and Stability of Phytate Complexes in Solution. *Coord. Chem. Rev.* **2008**, *252*, 1108–1120.

(25) Hong, D.-Y.; Hwang, Y. K.; Serre, C.; FÉrey, G.; Chang, J.-S. Porous Chromium Terephthalate MIL101 with Coordinatively Unsaturated Sites: Surface Functionalization, Encapsulation, Sorption, and Catalysis. *Adv. Funct. Mater.* **2009**, *19*, 1537–1552.

(26) Juan-Alcañiz, J.; Ramos-Fernandez, E. V.; Lafont, U.; Gascon, J.; Kapteijn, F. Building MOF Bottles around Phosphotungstic Acid Ships: One-Pot Synthesis of Bi-Functional Polyoxometalate-MIL-101 Catalysts. *J. Catal.* **2010**, *269*, 229–241.

(27) Férey, G.; Mellot-Draznieks, C.; Serre, C.; Millange, F.; Dutour, J.; Surble, S.; Margiolaki, I. A Chromium Terephthalate-Based Solid with Unusually Large Pore Volumes and Surface Area. *Science* **2005**, *309*, 2040–2042.

(28) Llewellyn, P. L.; Bourrelly, S.; Serre, C.; Vimont, A.; Daturi, M.; Hamon, L.; De Weireld, G.; Chang, J.-S.; Hong, D.-Y.; Hwang, Y. K.; Jung, S. H.; Férey, G. High Uptakes of CO_2 and CH_4 in Mesoporous Metal–Organic Frameworks MIL-100 and MIL-101. *Langmuir* **2008**, *24*, 7245–7250.

(29) Li, Z.; He, G. W.; Zhao, Y. N.; Cao, Y.; Wu, H.; Li, Y. F.; Jiang, Z. Y. Enhanced Proton Conductivity of Proton Exchange Membranes by Incorporating Sulfonated Metal–Organic Frameworks. *J. Power Sources* **2014**, *262*, 372–379.

(30) Gao, L.; Zhang, C.; Zhang, M.; Huang, X.; Jiang, X. Phytic Acid Conversion Coating on Mg–Li Alloy. *J. Alloys Compd.* **2009**, *485*, 789–793.

(31) Ponomareva, V. G.; Kovalenko, K. A.; Chupakhin, A. P.; Dybtsev, D. N.; Shutova, E. S.; Fedin, V. P. Imparting High Proton Conductivity to a Metal–Organic Framework Material by Controlled Acid Impregnation. *J. Am. Chem. Soc.* **2012**, *134*, 15640–15643.

(32) Sinha Ray, S.; Okamoto, M. Polymer/Layered Silicate Nanocomposites: A Review from Preparation to Processing. *Prog. Polym. Sci.* **2003**, *28*, 1539–1641.

(33) Zou, H.; Wu, S.; Shen, J. Polymer/Silica Nanocomposites: Preparation, Characterization, Properties, and Applications. *Chem. Rev.* **2008**, *108*, 3893–3957.

(34) Pichonat, T.; Gauthier-Manuel, B.; Hauden, D. A New Proton-Conducting Porous Silicon Membrane for Small Fuel Cells. *Chem. Eng. J.* **2004**, *101*, 107–111.

(35) Pereira, F.; Valle, K.; Belleville, P.; Morin, A.; Lambert, S.; Sanchez, C. Advanced Mesoporous Hybrid Silica-Nafion Membranes for High-Performance PEM Fuel Cell. *Chem. Mater.* **2008**, *20*, 1710–1718.

(36) Park, C. H.; Lee, C. H.; Guiver, M. D.; Lee, Y. M. Sulfonated Hydrocarbon Membranes for Medium-Temperature and Low-Humidity Proton Exchange Membrane Fuel Cells (PEMFCs). *Prog. Polym. Sci.* **2011**, *36*, 1443–1498.

(37) Jeong, N. C.; Samanta, B.; Lee, C. Y.; Farha, O. K.; Hupp, J. T. Coordination-Chemistry Control of Proton Conductivity in the Ionic Metal–Organic Framework Material HKUST-1. *J. Am. Chem. Soc.* **2012**, *134*, 51–54.

(38) Wu, B.; Lin, X.; Ge, L.; Wu, L.; Xu, T. A Novel Route for Preparing Highly Proton Conductive Membrane Materials with Metal–Organic Frameworks. *Chem. Commun.* **2013**, *49*, 143–145.